

Mixed Convection Flow and Heat Transfer of Micropolar Fluid in a Vertical Channel with Symmetric and Asymmetric Wall Heating Conditions

Patil Mallikarjun B¹, Chandrali Baishya²

Department of Studies and Research in Mathematics, Tumkur University, Tumkur-572 103, Karnataka, India

ABSTRACT

Analytical solutions for fully developed mixed convection flow of a micro polar fluid with heat generation or heat absorption in a parallel plate vertical channel with symmetric and asymmetric wall temperature distribution has been presented. The two boundaries of the channel are kept either at equal or at different temperatures as isothermal-isothermal, isoflux-isothermal and isothermal-isoflux cases. Reverse flow conditions are observed with increase in micro vortex viscosity. Micro polar fluids display reduction in heat transfer rate.

Key Words: *Mixed convection, Viscous Dissipation and Micropolar fluid.*

I. INTRODUCTION

The theory of micropolar and thermomicropolar fluids formulated by Eringen [1,2] has shown much interest in recent years because of its considerable attention due to there application in a number of processes that occur in industry. The applications include the extrusion of polymer fluids, solidification of liquid crystals, cooling of a metallic plate in a bath, animal blood, exotic lubricants and in colloidal suspensions. A detailed review of the published papers on these fluids can be found in the review article by Arimal et al. [3,4] and Eringen [5].

The essence of the theory of micropolar fluid flow lies in the extension of the constitutive equations for Newtonian fluids so that more complex fluids can be described by this theory. In this theory, the rigid particles contained in as small fluid volume element are limited to rotation about the center of the volume elements described by the micro rotation vector. Such fluids display the effects of local rotary inertia and couple stresses.

Further the desired model of the non-Newtonian flow of fluids containing microconstituents motivated the development of the theory. Subsequent studies have successfully applied the model to a wide range of applications including blood flows, porous media, lubricants, turbulent shear flows, flow in capillaries and micro channels etc.

The interest in heat transfer problems involving non-Newtonian fluids has grown persistently in the past half century. Hinch [6] has given an excellent sequence of lectures on non-Newtonian fluids. Many practical applications of mixed convection exists, including in the fuel element of a nuclear reactor, in the heaters and coolers of mechanical or chemical devices, in the lubrication of machine parts etc. Chiu et.al [7] studied the effect of microstructure on the free convection heat transfer in enclosures. Chamkha, Grosan and Pop [8] studied both analytically and numerically the problem of fully developed free convection flow of a micropolar fluid between a parallel plate vertical channel with asymmetric wall distribution. Again the same authors in [9] studied the fully developed flow of a micropolar fluid in a mixed convection between a parallel-plate vertical channel with asymmetric wall temperature distribution. They observed flow reversal due to buoyancy force and they also derived criteria for the occurrence of the flow. Buoyancy and wall conduction effects on forced convection of micropolar fluid flow along a vertical slender flow circular cylinder have been studied by Cheng et.al [10].

However, the effect of heat absorption or heat generation on the mixed convection flow and heat transfer of a micropolar fluid in vertical channel geometry with symmetric and asymmetric wall conditions has not been studied. The aim of the present study is to discuss such situation. It is also of our interest to investigate the effect of material constant on the micropolar fluid on the flow and heat transfer through vertical channel with symmetric and asymmetric wall heating conditions with heat generation or heat absorption coefficient for three thermal boundary conditions.

II. BASIC EQUATIONS

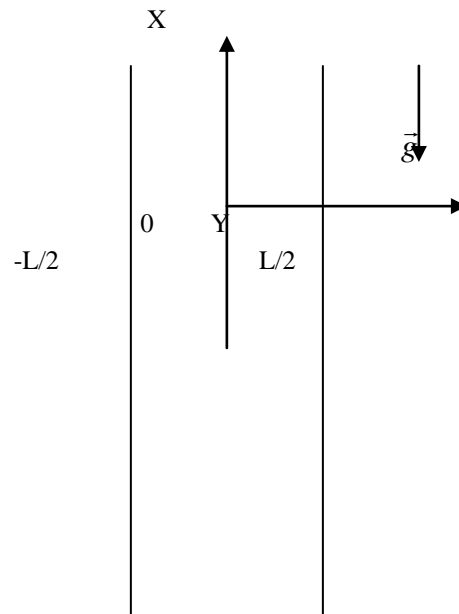


FIG. 1
 Physical configuration

Consider steady, laminar, micropolar fully developed flow with heat generation and heat absorption in a parallel plate vertical channel, the physical configuration is shown in figure 1. The flow is assumed to be steady and fully developed.

The oberbeck –Boussinesq approximation is assumed to hold good for the evaluation of the gravitational body force. Hence, the density will depend on temperature according to the equation of state

$$\text{For the fully developed flow, we have } \frac{\partial U}{\partial X} = 0. \quad (1)$$

Since the velocity field U is solenoidal, one obtains $\frac{\partial V}{\partial Y} = 0$. As a consequence, the velocity component V is constant in any channel section and is equal to zero at the channel walls, so that V must be vanishing at any position. The Y -momentum balance equation can be expressed as $\frac{\partial P}{\partial Y} = 0$ where

$P = p + \rho_0 g X$ is the difference between the pressure and the hydrostatic pressure. Therefore P depends only on X and the Y momentum balance equation is given by Chamkha et.al (2003) as

$$\rho_0 g \beta (T - T_0) - \frac{dP}{dX} + (\mu + k) \frac{d^2 u}{dy^2} + k \frac{d\bar{N}}{dY} = 0 \quad (2)$$

$$\gamma \frac{d^2 \bar{N}}{dY^2} - 2k \bar{N} - k \frac{dU}{dY} = 0 \quad (3)$$

We assume that the walls of the channel are isothermal, the boundaries temperatures are T_1 at $Y = -L/2$ and T_2 at $Y = L/2$ with $T_2 \geq T_1$.

Here, N is the microrotation component of micropolar fluid normal to (x,y) plane.

Comparing these boundary conditions with momentum equation (2) we see for the compatibility that $\frac{dP}{dX}$ should be independent of X and hence there exists a constant A such that

$$\frac{dP}{dX} = A \quad (4)$$

The energy balance equation is given by (neglecting viscous dissipation)

$$K \frac{d^2T}{dY^2} \pm Q(T - T_0) = 0 \quad (5)$$

The corresponding boundary conditions are given by

$$U\left(\pm \frac{L}{2}\right) = \bar{N}\left(\pm \frac{L}{2}\right) = 0 \quad (6)$$

and

$$U\left(\pm \frac{L}{2}\right) = \pm \frac{R_T}{2} \quad (7)$$

The above equations (2), (3), (5) and (6) can be written in dimensionless form by using the dimensionless quantities

$$\begin{aligned} u &= \frac{U}{U_0}; & y &= \frac{Y}{D}; & j &= D^2; & k &= \mu K_1; & \bar{N} &= \frac{U_0}{D} N \\ \text{Re} &= \frac{U_0 D}{\nu}; & \text{Pr} &= \frac{\nu}{\alpha}; & \gamma &= (\mu + k/2); & \phi &= \frac{QD^2}{K}; \\ \text{Gr} &= \frac{g \beta \Delta T D^3}{\nu^2}; & \lambda &= \frac{Gr}{\text{Re}}; & R_T &= \frac{T_2 - T_1}{\Delta T}; & \theta &= \frac{T - T_0}{\Delta T} \end{aligned} \quad (8)$$

The diameter of the channel is given by $D = 2L$ and U_0, T_0 are the corresponding reference velocity and reference temperature given by

$$U_0 = -\frac{AD^2}{48\mu}; \quad T_0 = \frac{T_1 + T_2}{2}. \quad (9)$$

The temperature difference ΔT is given by

$$\Delta T = T_2 - T_1 \text{ if } T_1 < T_2 \text{ and } \Delta T = \frac{\nu^2}{C_p D^2} \text{ if } T_1 = T_2. \quad (10)$$

The dimensionless parameter R_T is zero for symmetric heating ($T_1 = T_2$) and R_T is one for asymmetric heating ($T_1 < T_2$)

Using equation (9) equations (2), (3), (5) and (6) reduces to

$$(1 + K_1) \frac{d^2u}{dy^2} + K_1 \frac{dN}{dy} + \lambda\theta + 48 = 0 \quad (11)$$

$$\left(1 + \frac{K_1}{2}\right) \frac{d^2N}{dy^2} - 2K_1N - K_1 \frac{du}{dy} = 0 \quad (12)$$

$$\frac{d^2\theta}{dy^2} \pm \phi\theta = 0 \quad (13)$$

$$u\left(\pm \frac{1}{4}\right) = N\left(\pm \frac{1}{4}\right) = 0 \quad (14)$$

and

$$\theta\left(\pm \frac{1}{4}\right) = \pm \frac{R_T}{2} \quad (15)$$

The solution of equation (13) by using the boundary condition (15) are given by

$$\theta = \frac{R_T}{2} \frac{\text{Sin}(\sqrt{\phi} y)}{\text{Sin}(\sqrt{\phi} / 4)} \quad (16)$$

for the case of heat generation and

$$\theta = \frac{R_T}{2} \frac{\text{Sinh}(\sqrt{\phi} y)}{\text{Sinh}(\sqrt{\phi} / 4)} \quad (17)$$

for the case of heat absorption. Integrating the equation (10) with respect to y than by using equations (15) and (16) we get

$$\frac{du}{dy} = -\frac{K_1}{(1+K_1)} N + \frac{\lambda R_T}{2\sqrt{\phi}(1+K_1)\text{Sin}\sqrt{\phi}/4} \text{Cos}\sqrt{\phi}y - \frac{48}{(1+K_1)} y - \frac{B}{(1+K_1)} \quad (18)$$

for the case of heat generation and

$$\frac{du}{dy} = -\frac{K_1}{(1+K_1)} N - \frac{\lambda R_T}{2\sqrt{\phi}(1+K_1)\text{Sinh}\sqrt{\phi}/4} \text{Cosh}\sqrt{\phi}y - \frac{48}{(1+K_1)} y - \frac{B}{(1+K_1)} \quad (19)$$

for the case of heat absorption.

Substituting equations (18) and (19) in equation (12) we get

$$\frac{d^2N}{dy^2} - \tau N = \frac{\lambda K_1 R_T}{\sqrt{\phi}(1+K_1)(2+K_1)\text{Sin}\sqrt{\phi}/4} \text{Cos}\sqrt{\phi}y - \frac{48\tau}{(2+K_1)} y - \frac{B\tau}{(2+K_1)} \quad (20)$$

for the case of heat generation and

$$\frac{d^2N}{dy^2} - \tau N = -\frac{\lambda K_1 R_T}{\sqrt{\phi}(1+K_1)(2+K_1)\text{Sinh}\sqrt{\phi}/4} \text{Cosh}\sqrt{\phi}y - \frac{48\tau}{(2+K_1)} y - \frac{B\tau}{(2+K_1)} \quad (21)$$

for the case of heat absorption.

By using the boundary condition (14), the solutions of above equation (20) and (21) are

$$N = C_3 \text{Cosh}\sqrt{\tau}y + C_4 \text{Sinh}\sqrt{\tau}y + l_1 \text{Cos}\sqrt{\phi}y + l_2 y + l_3 \quad (22)$$

for the case of heat generation and

$$N = C_3 \text{Cosh}\sqrt{\tau}y + C_4 \text{Sinh}\sqrt{\tau}y + l_1 \text{Cosh}\sqrt{\phi}y + l_2 y + l_3 \quad (23)$$

for the case of heat absorption.

Differentiating the above equations (22) and (23) with respect to y and than by using equations (16) and (17) and integrating equation (11) two times with respect to y we get

$$u = -\frac{1}{(1+K_1)} \left(\frac{C_3 K_1}{\sqrt{\tau}} \text{Sinh}\sqrt{\tau}y + \frac{C_4 K_1}{\sqrt{\tau}} \text{Cosh}\sqrt{\tau}y + \left(\frac{l_1 K_1}{\sqrt{\phi}} - \frac{\lambda R_T}{2\phi \text{Sin}\sqrt{\phi}/4} \right) \text{Sin}\sqrt{\phi}y \right) \left((48+l_2 K_1) \frac{y^2}{2} + C_5 y + C_6 \right) \quad (24)$$

for the case of heat generation and

$$u = -\frac{1}{(1+K_1)} \left(\frac{C_3 K_1}{\sqrt{\tau}} \text{Sinh}\sqrt{\tau}y + \frac{C_4 K_1}{\sqrt{\tau}} \text{Cosh}\sqrt{\tau}y + \left(\frac{l_1 K_1}{\sqrt{\phi}} + \frac{\lambda R_T}{2\phi \text{Sinh}\sqrt{\phi}/4} \right) \text{Sinh}\sqrt{\phi}y \right) \left((48+l_2 K_1) \frac{y^2}{2} + C_5 y + C_6 \right) \quad (25)$$

for the case of heat absorption.

Again differentiating the equations (24) and (25) with respect to y and comparing with equations (18) and (19) we get the value of constant B for both cases of heat generation and heat absorption is

$$B = \frac{C_5(2 + K_1)}{2(1 + K_1)} \quad (26)$$

isoflux-isothermal walls ($q_1 - T_2$)

The dimensional forms of thermal boundary condition for the channel walls are

$$q_1 = -k \left. \frac{dT}{dY} \right|_{-\frac{L}{2}}; \quad T\left(\frac{L}{2}\right) = T_2 \quad (27)$$

The dimensionless form of equation (27) can be obtained by using equation (8) with $\Delta T = q_1 D/k$ to give

$$\left. \frac{d\theta}{dy} \right|_{-\frac{1}{4}} = -1; \quad \theta\left(\frac{1}{4}\right) = R_{qt} \quad (28)$$

Where $R_{qt} = (T_2 - T_0) / \Delta T$ is the thermal ratio parameter for the isoflux-isothermal case.

The solutions of temperature, micro rotation velocity and velocity are obtained from eqs. (11) – (13) by using the boundary conditions (14) & (28).

$$\begin{aligned} \theta &= C_1 \cos\sqrt{\phi}y + C_2 \sin\sqrt{\phi}y \\ N &= C_3 \cosh\sqrt{\tau}y + C_4 \sinh\sqrt{\tau}y + l_1 \sin\sqrt{\phi}y + l_2 \cos\sqrt{\phi}y + l_3 y + l_4 \\ u &= -\frac{1}{(1 + K_1)} \left(\begin{aligned} &\left(\frac{C_3 K_1}{\sqrt{\tau}} \sinh\sqrt{\tau}y + \frac{C_4 K_1}{\sqrt{\tau}} \cosh\sqrt{\tau}y - \left(\frac{l_1 K_1}{\sqrt{\phi}} - \frac{\lambda C_1}{\phi} \right) \cos\sqrt{\phi}y + \right. \\ &\left. \left(\frac{l_2 K_1}{\sqrt{\phi}} - \frac{\lambda C_2}{\phi} \right) \sin\sqrt{\phi}y + (48 + l_3 K_1) \frac{y^2}{2} + C_5 y + C_6 \right) \end{aligned} \right) \end{aligned} \quad (29)$$

for the case of heat generation and

$$\begin{aligned} \theta &= C_1 \cosh\sqrt{\phi}y + C_2 \sinh\sqrt{\phi}y \\ N &= C_3 \cosh\sqrt{\tau}y + C_4 \sinh\sqrt{\tau}y + l_1 \sinh\sqrt{\phi}y + l_2 \cosh\sqrt{\phi}y + l_3 y + l_4 \\ u &= -\frac{1}{(1 + K_1)} \left(\begin{aligned} &\left(\frac{C_3 K_1}{\sqrt{\tau}} \sinh\sqrt{\tau}y + \frac{C_4 K_1}{\sqrt{\tau}} \cosh\sqrt{\tau}y + \left(\frac{l_1 K_1}{\sqrt{\phi}} + \frac{\lambda C_1}{\phi} \right) \cosh\sqrt{\phi}y + \right. \\ &\left. \left(\frac{l_2 K_1}{\sqrt{\phi}} + \frac{\lambda C_2}{\phi} \right) \sinh\sqrt{\phi}y + (48 + l_3 K_1) \frac{y^2}{2} + C_5 y + C_6 \right) \end{aligned} \right) \end{aligned} \quad (30)$$

for the case of heat absorption.

isothermal-isoflux walls ($T_1 - q_2$)

The results are same as we obtained in the case of isoflux-isothermal case with constant $-C_1$ replaced by C_1 .

III. RESULTS AND DISCUSSION

For various parametric values, the velocity and microrotation is drawn in figures 2 to 19.

From figure 2, we notice that the velocity shows a decreasing tendency with increase in K_1 with the material parameter for $\lambda = 100$, $\phi = 5$ (heat generation parameter), $R_t = 1$. Further for $\lambda = -100$, we observe that the velocity profiles tend to be asymmetric i.e., the velocity profiles are towards the left of the centre of the channel and for $\lambda = 100$, they are towards the right of the channel.

The effect of material parameters K_1 on micro rotation is drawn in Figure 3. We observed that with increase in K_1 micro rotation is reversed on the range -0.25 to 0 and it is increasing on the range 0 to 0.25. The point of inflexion occurs at $y = 0.5$.

In Figure 4, the flow velocity shows a reversal tendency with increase in λ near the wall $y = -1/4$ and decreases at the right wall $y = 1/4$ as K_1 increases. Hence the effect of K_1 is to decrease the flow velocity in both cases.

In Figure 5, the magnitude of reversal in micro rotation is large in the region from $y = 0$ to 0.16 with increase in K_1 and for $\lambda = 500$. The point of inflexion shifts to $y = 0.16$ For $\lambda = -500$ the micro rotation shows an increasing behavior with increase in K_1 . Thus increase in K_1 leads to the vertex viscosity being dominant than the fluid viscosity and however, with increase in buoyancy force the micro rotation decrease. Thus, buoyancy force results in decrease of micro rotation.

From Figure 6, we observe that with increase in ϕ and $\lambda = 500$, the flow velocity is reversal near the left wall and increases as we move towards right wall. However, with increase in K_1 the flow velocity decreases along with decreases in flow reversal. The same nature is observed for neighboring values of λ (buoyancy parameters).

Figure 7 shows the behavior of micro rotation for various values of λ , ϕ and K_1 . We observe that with increase in ϕ , the micro rotation decreases when $\lambda = 500$ and it increases when $\lambda = -500$. Thus, the buoyancy force decreases the micro rotation ($\lambda = 500$) and when it is weaker ($\lambda = -500$), it supports increases on micro rotation.

The plots of u and micro rotation N are plotted in fig.8 and 9 for the case of isoflux-isothermal temperature distribution. For both Newtonian and micropolar fluids, the effect of heat generation parameter ' ϕ ' is to increase velocity for $\lambda = 500$. The microrotation decreases with increase in ' ϕ ' in the first half portion while it increases for

$\phi = -500$ in the same region. The reverse behavior is observed in the second half portion giving rise to a point of inflexion at (0, 0) as can be seen from fig.9. It is interesting to see that for the case of isothermal-isoflux wall condition, the above behavior is interchanged as seen from fig.10 and 11.

The effect of material parameter K_1 on velocity and microrotation velocity is shown in figures 12 and 13, for symmetric heating. As K_1 increases velocity decreases. The effect of K_1 on microrotation velocity is to increase the microrotation velocity in the range of y from 0 to 0.25 and decrease in the range from -0.25 to 0 for $\lambda = \pm 500$

The effect of heat absorption coefficient ϕ and K_1 are shown in Figure 14 to 19 for isoflux-isothermal and isothermal-isoflux wall conditions on velocity and microrotation velocity. Figure 14 shows that as ϕ increases velocity decreases for Newtonian and micropolar fluid for $\lambda = \pm 500$. Figure 15 shows that as ϕ increases microrotation velocity decreases for $\lambda = 500$ and increases for $\lambda = -500$.

The effect of ϕ is to decrease the velocity for Newtonian and micropolar fluid for $\lambda = 500$ and increases the velocity for $\lambda = -500$ for isoflux-isothermal wall conditions as seen in Figure 16. It is seen from Figure 17 that

microrotation velocity N decreases as ϕ increases for $\lambda = -500$ and increases for $\lambda = 500$, for isoflux-isothermal wall conditions. The effect of ϕ and K_1 on velocity and microrotation velocity remains the same for isothermal-isoflux wall conditions by interchanging λ are shown in figures 18 and 19.

Nomenclature

A, B	constant defined in equation (4)
C_p	specific heat at constant pressure
D	$= 2L$, hydraulic diameter
g	acceleration due to gravity
λ	dimensionless parameter (Gr/Re) defined in equation (8)
Gr	Grashof number defined in equation (8)
K	thermal conductivity
K_1	non-dimensional material parameter
L	channel width
N	microrotation
p	pressure
P	$= p + \rho_o g X$, difference between the pressure and the hydrostatic pressure
Re	Reynolds number defined in equation (8)
R_T	temperature difference ratio defined in equation (8)
T	temperature
T_1, T_2	prescribed boundary temperatures
T_o	reference temperature
u	dimensionless velocity component in the X- direction
U	velocity component in the X-direction
U_o	reference velocity defined in equation (8)
V	velocity component in the Y-direction
X, Y	space coordinates
y	dimensionless transverse coordinate

Greek symbols

α	$= \frac{k}{\rho_o C_p}$, thermal diffusivity
β	thermal expansion coefficient
γ	spin-gradient viscosity
k	vortex viscosity
ΔT	reference temperature difference defined by equation (10)
θ	dimensionless temperature defined in equation (8)
μ	dynamic viscosity
ν	$= \frac{\mu}{\rho_o}$, kinematic viscosity

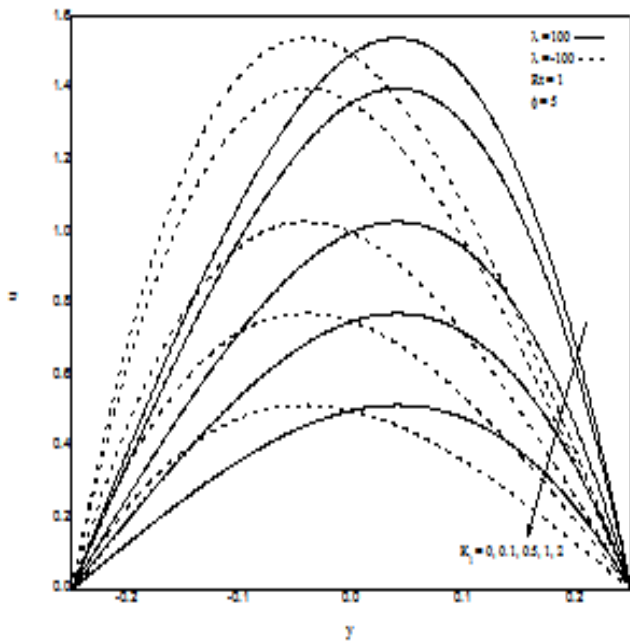


FIG. 2

Plots of u versus y in the case of asymmetric heating for different values of λ and K_1

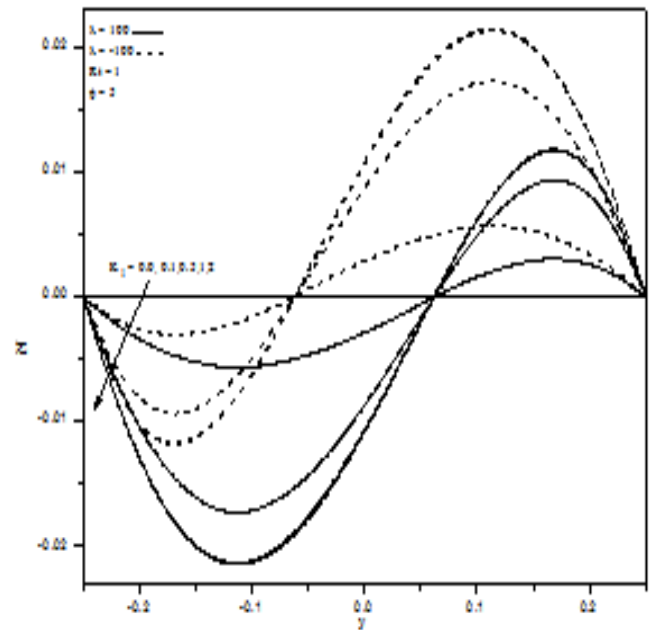


FIG. 3

Plots of N versus y in the case of asymmetric heating for different values of λ and K_1

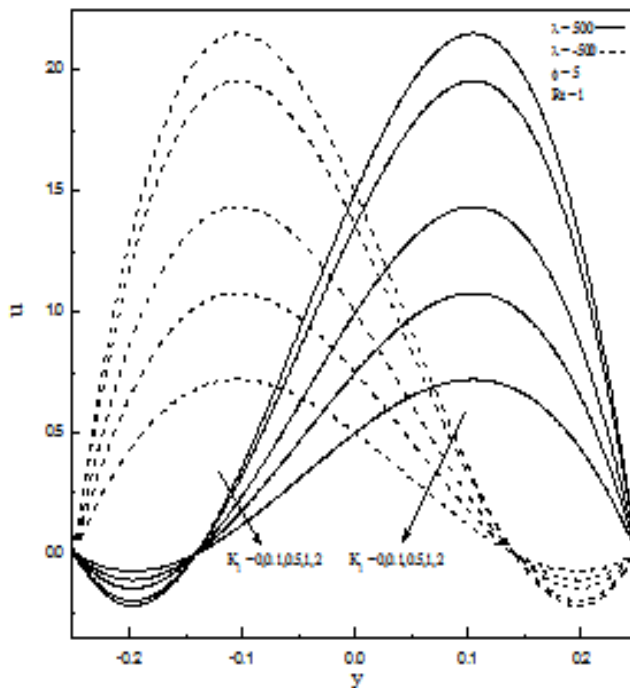


FIG. 4

Plots of u versus y in the case of asymmetric heating for different values of λ and K_1

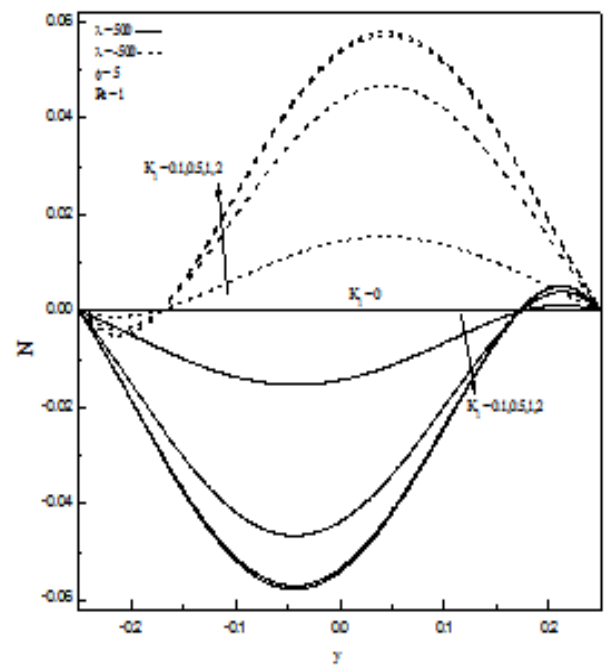


FIG. 5

Plots of N versus y in the case of asymmetric heating for different values of λ and K_1

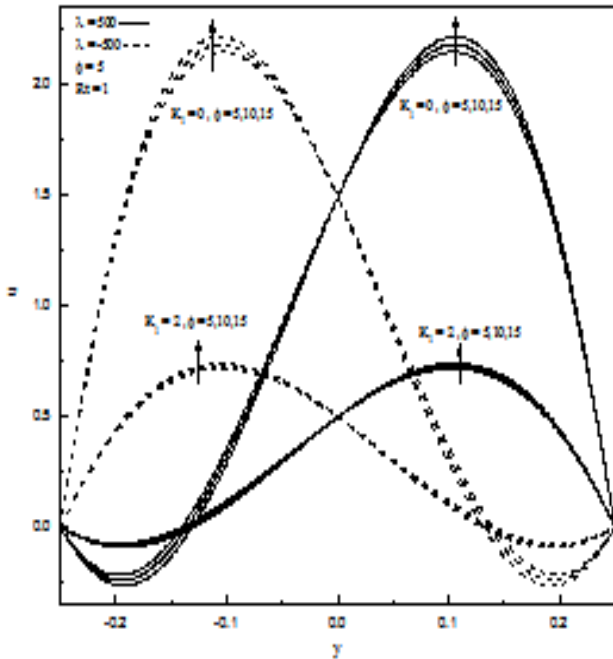


FIG 6
 Plots of u versus y in the case of asymmetric heating
 for different values of heat generation coefficient θ and K_1

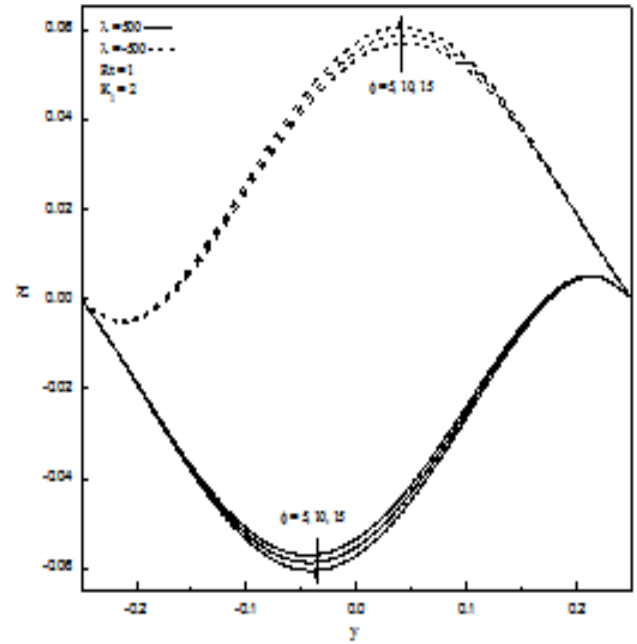


FIG 7
 Plots of N versus y in the case of asymmetric heating
 for different values of heat generation coefficient θ and K_1

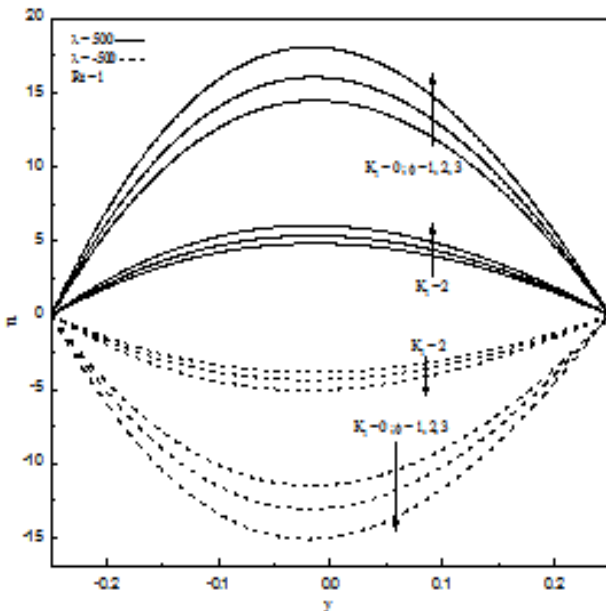


FIG 8
 Plots of u versus y for different values of heat generation
 coefficient θ and K_1 for isoflux-isothermal case

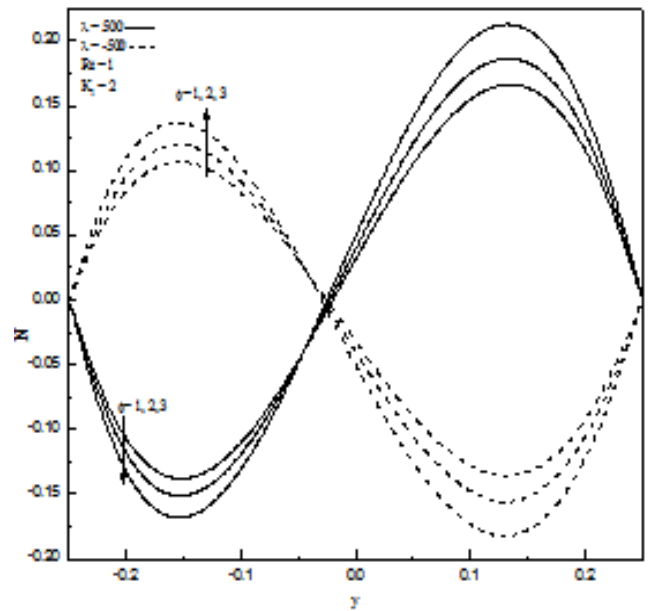


FIG 9
 Plots of N versus y for different values of heat
 generation coefficient θ for isoflux-isothermal case

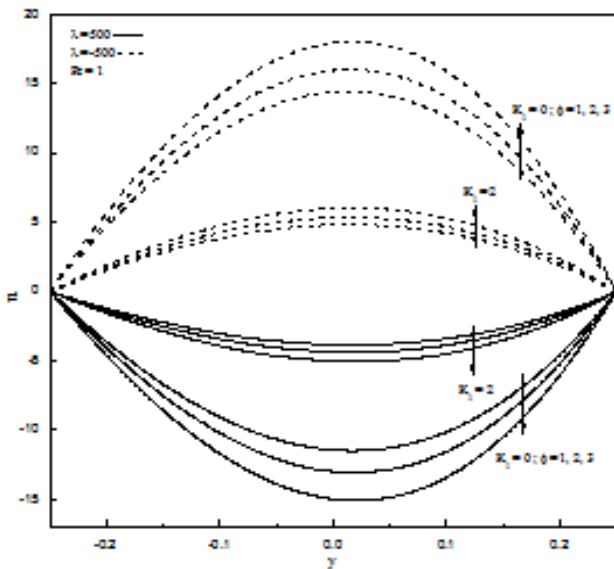


FIG. 10
 Plots of u versus y for different values of heat generation coefficient ϕ and K_1 for isothermal-isoflux case

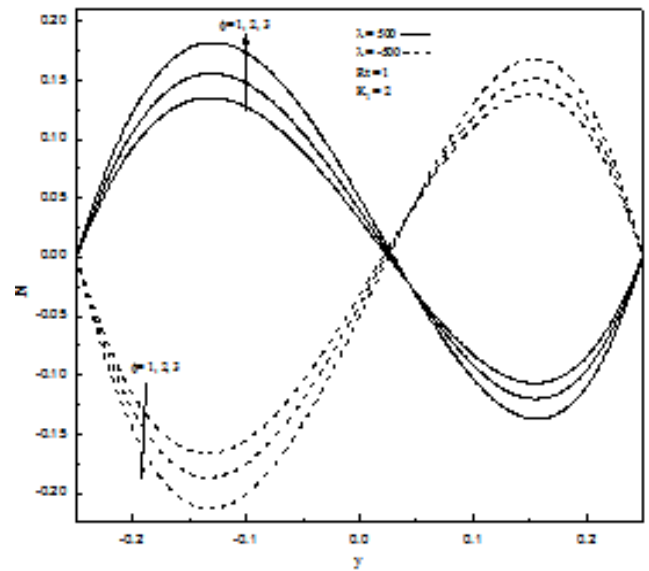


FIG. 11
 Plots of N versus y for different values of heat generation coefficient ϕ for isothermal-isoflux case

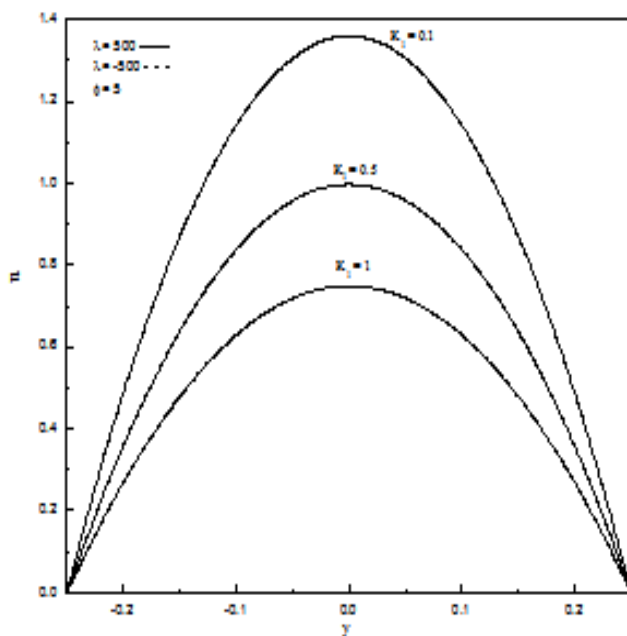


FIG. 12
 Plots of u versus y in the case of symmetric heating for different values of values of K_1

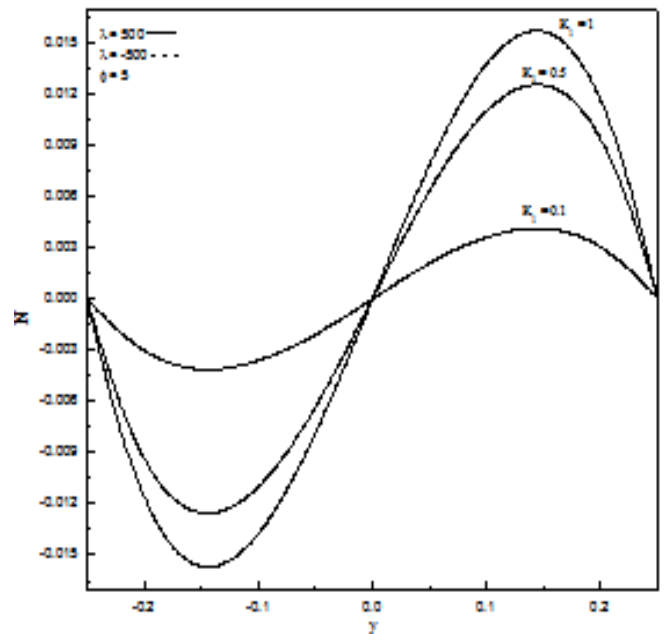


FIG. 13
 Plots of N versus y in the case of symmetric heating for different values of values of K_1

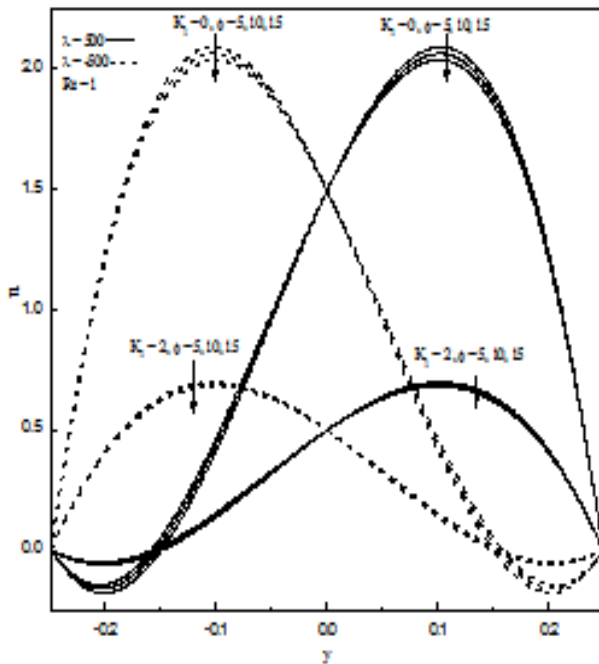


FIG. 14
 Plots of u versus y in the case of asymmetric heating for different values of heat absorption coefficient ϕ and K_1

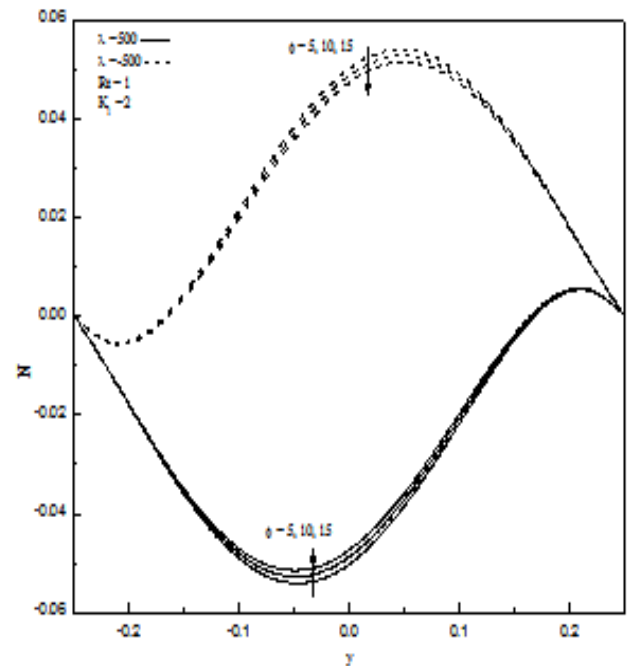


FIG. 15
 Plots of N versus y in the case of asymmetric heating for different values of heat absorption coefficient ϕ and K_1

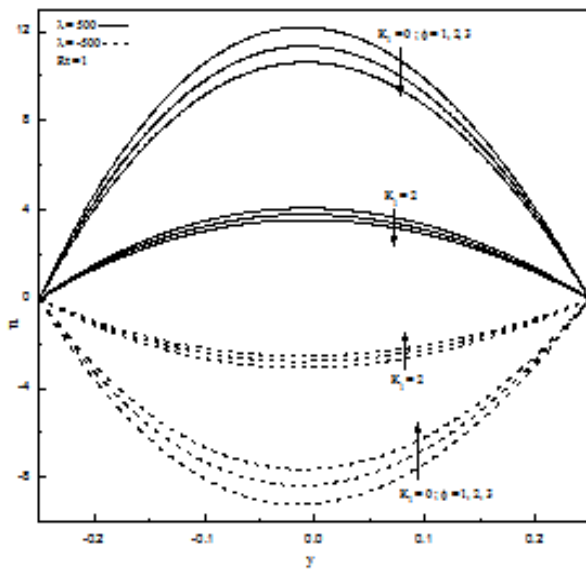


FIG. 16
 Plots of u versus y for different values of heat absorption coefficient ϕ and K_1 for isoflux-isothermal case

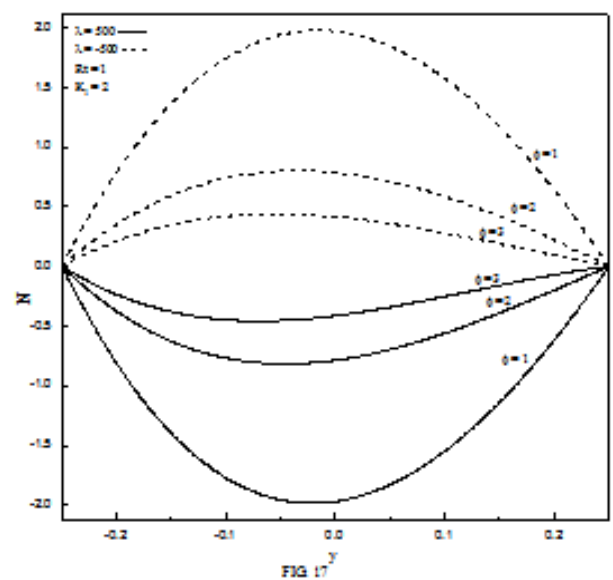


FIG. 17
 Plots of N versus y for different values of heat absorption coefficient ϕ for isoflux-isothermal case

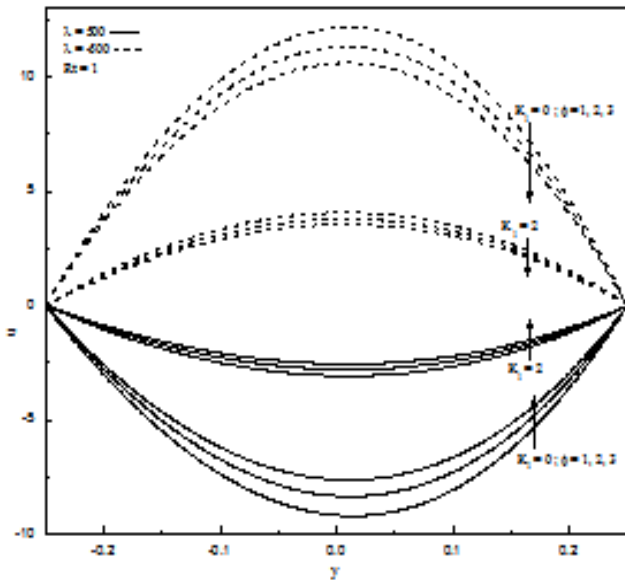


FIG. 18
 Plots of u versus y for different values of heat absorption coefficient ϕ and K_1 , for isothermal-isoflux case

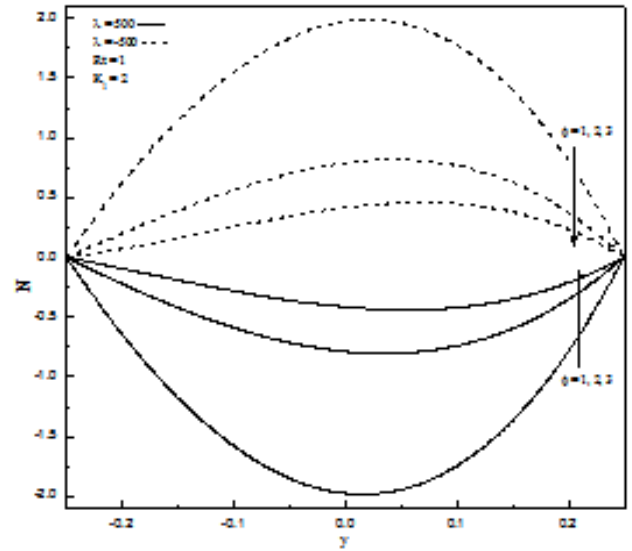


FIG. 19
 Plots of N versus y for different values of heat absorption coefficient ϕ , for isothermal-isoflux case

REFERENCES

- [1] A C Eringen, *Int.J.Engg.Sci.*,1964,2,205
- [2] A C Eringen, *Int.J.Engg.Sci.*,1969,7,115
- [3] T Arimen, M A Turk and M D Sylvester, *Int.J.Engg.Sci.*,1974,12,273
- [4] T Arimen, M A Turk and M D Sylvester/*J/ Int.J.Engg.Sci.*, 1973, 11, 905
- [5] A C Eringen, *Journal of Math Mech.*1966, 16,1
- [6] J Hince, Non-Newtonian geophysical fluid dynamics. Woods hole Oceanographic Inst. Woods Hole, MA02543, USA,2003.
- [7] C P Chiu, J Y Shin and W R Chen,*Acta Mechanica*, 132, 75 , 1999.
- [8] A J Chamka, Grosan and I Pop, Fully developed convection of a micropolar fluid in a vertical channel, *Int. Comm. Heat and Mass transfer* 29(8), 1119, 2002.
- [9] A J Chamka, Gronan and I Pop, Fully developed convection of a micropolar fluid in a vertical channel, *Int.J.Fluid Mechanics Res*,30(3), 2003.
- [10] Cheng-Longchang, Buoyance and wall conduction effects on forced convection of Micropolar fluid flow along a vertical slender hollow circular cylinder. *Int.J.Heat and Mass trans.* 49, 4932, 2006.